SHEAR BEHAVIOR OF URM RETROFITTED WITH FRP OVERLAYS

By M. R. Ehsani,[1] Member, ASCE, H. Saadatmanesh,[2] Member, ASCE, and A. Al-Saidy[3]

ABSTRACT: A large inventory of older masonry buildings exists in earthquake-prone regions. In most cases these buildings contain shear walls constructed of unreinforced masonry. The majority of these buildings were built before any provisions for earthquake loadings were established. The failures and damages reported in recent earthquakes attest to the need for efficient strengthening procedures. The effectiveness of increasing the shear strength of brick masonry by epoxy-bonding fiber-reinforced polymer (FRP) overlays to the exterior surfaces was evaluated. The variables in the test included the strength of the composite fabric, fiber orientation, and anchorage length. The specimens were tested under static loading. The results showed that both the strength and ductility of tested specimens were significantly enhanced with this technique. The orientation of the angle of fibers with respect to the plane of loading had a major effect on the stiffness of the retrofitted system but did not affect the ultimate strength significantly.

INTRODUCTION

General

Masonry structures have been constructed since the earliest days of civilization. They still constitute a significant percentage of the current building stock. Many of these buildings are located in seismic regions and were built before the establishment of any building-code requirements for earthquake-resistant construction. These structures are usually constructed from concrete blocks or clay bricks. The block or brick units are tied together by a cement mortar; little or no steel is used in these structures. In fact, it has been reported that the use of steel as reinforcement for masonry structures was introduced in the United States in the 1930s to the 1940s (Amhein 1992). While properly reinforced masonry structures can and do perform well during earthquakes, the lack of reinforcement in the large inventory of existing masonry buildings is a major concern of the profession.

Masonry buildings consist of several structural element types. However, the one most likely to be subjected to earthquake damages is the load-bearing wall. These elements are designed primarily to resist vertical (axial) loads. However, they are often subjected to in-plane or out-of-plane loads resulting from lateral loads such as earthquakes. Many of the older masonry buildings are unreinforced, and are commonly referred to as unreinforced masonry (URM) buildings. The in-plane (shear) resistance in load-bearing URM walls is provided by the shear bond strength of the mortar and the friction shear due to the vertical load. The aging and often deteriorated mortar joints have little shear capacity. Under severe earthquake loads the shear capacity of the mortar is exceeded, resulting in failure of the wall. Thus, effective techniques are needed to strengthen such walls.

Modes of Failure

Chen and Shah (1988) have shown that the mode of failure of a single pier [0.25 scale, 274 × 256 × 14 mm (10.75 × 10.1 × 0.56 in.)] subjected to dynamic loading is characterized by horizontal cracks going through the toe of the pier. Shear slip along the horizontal cracks were observed during the dynamic shaking test. In addition, Abrams (1992) has reported on tests of a series of unreinforced walls. Two of the walls were built using reclaimed Chicago common bricks from a building that was built in 1917. The length-to-height aspect ratio of the two walls and the vertical compressive stress varied so that two different behavioral modes could be observed. The first wall had an aspect ratio of 2.0 and was subjected to a vertical stress of 0.52 MPa (75 psi). This wall failed in shear (diagonal tension) with no flexural cracking. The second wall had an aspect ratio of 1.5, and was subjected to a stress of 0.34 MPa (50 psi). This wall, which was subjected to a smaller vertical compressive stress, cracked initially in flexure (horizontal cracks). The preceding review indicates that the type of failure depends on the geometry of the structural element and the loading combination.

According to Drysdale et al. (1979, 1994), depending on the form of construction and the combined effects of axial load and bending, the shear failure mode is characterized by:

- Shear slip along the bed joints
- Diagonal tension cracking
- Shear compression failure

These failure modes are shown in Fig. 1. Of these, the first two modes are the most common. In older URM buildings, the joints are the weakest part of the wall. Even in the case of diagonal tension cracking, the failure in most cases occurs by separation of the head joint and slip along the bed joints (i.e., step cracking). Thus, in both failure modes, a slip occurs along the bed joint and the strength of the bed joint controls the failure pattern. Even though a bed joint shear test can be generalized for both failure modes, the results of this study will be limited to the first failure mode (shear slip along the bed joints) as the type of testing conducted is directly related to this failure mode. Lenczer (1972) has reported that the shear strength of a bearing wall, in the case of slip failure mode, can be calculated as

$$\tau_b = \nu_{b0} + \mu\sigma_y \tag{1}$$

where τ_b = shear stress at the shear bond failure; ν_{b0} = shear bond strength at zero normal stress due to the adhesive strength of mortar; μ = coefficient of friction between brick and mortar; and σ_y = normal stress.

Review of Retrofitting Techniques

Several procedures have been used in the past to retrofit load-bearing walls. Two of these procedures have received considerable attention. The first involves removing one or

[1]Prof., Dept. of Civ. Engrg. and Engrg. Mech., The Univ. of Arizona, Tucson, AZ 85721.

[2]Assoc. Prof., Dept. of Civ. Engrg. and Engrg. Mech., The Univ. of Arizona, Tucson, AZ.

[3]Grad. Student, Dept. of Civ. Engrg. and Engrg. Mech., The Univ. of Arizona, Tucson, AZ.

Note. Discussion open until July 1, 1997. To extend the closing date one month, a written request must be filed with the ASCE Manager of Journals. The manuscript for this paper was submitted for review and possible publication on April 26, 1996. This paper is part of the *Journal of Composites for Construction*, Vol. 1, No. 1, February 1997. ©ASCE, ISSN 1090-0268/97/0001-0017–0025/$4.00 + $.50 per page. Paper No. 13124.

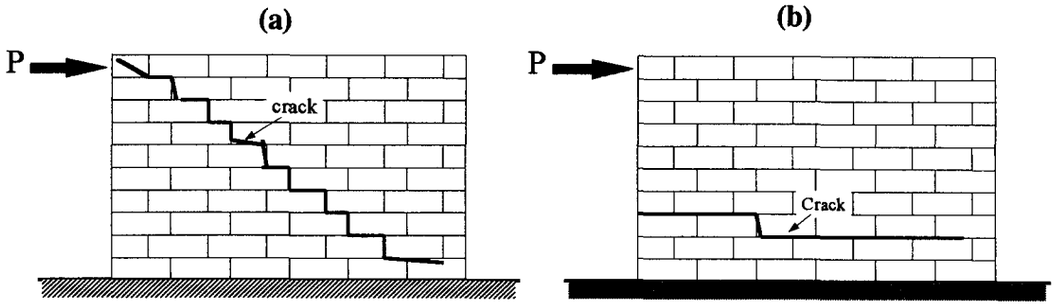

FIG. 1. Modes of Failure in URM Wall Subjected to Lateral Load P: (a) Diagonal Tension Cracking; (b) Slip along Bed Joint

more wythes of masonry and replacing the volume with a heavy coat of pneumatically applied concrete (Khan 1984). Although this technique is effective, it requires a great deal of surface preparation and formwork and adds considerable weight to the structure, which results in a higher inertia force in the event of an earthquake. Moreover, the additional weight added to the wall may necessitate foundation adjustments.

The second technique involves application of an external coating or overlay (surface treatment) to one or both sides of the masonry wall. This includes the use of sprayed concrete, glass-reinforced concrete coating, steel-fiber-reinforced concrete coating or ferrocement coatings (Reinhorn et al. 1985; Prawl et al. 1986). This procedure was found to be effective in recovering the original in-plane shear strength of damaged sections and in some cases doubled the in-plane shear strength of undamaged sections. Numerous studies (Jabarov et al. 1980; Sheppard and Tercelj 1980) on the in-plane strength of shear walls using mesh-reinforced mortar coatings indicate that the strengthened specimens were able to develop at least twice the strength of the unreinforced wall. Although effective, this procedure is usually accompanied with a great deal of disturbance to the occupants while the structure is undergoing rehabilitation.

Retrofit Using FRP

The use of fiber reinforced polymer (FRP) composites in civil engineering application has grown very rapidly in recent years. Composite materials essentially consists of a resin matrix reinforced with carbon, glass, or aramid fibers. Fibers are the elements that carry the load and the resin matrix ensures distribution of load among the fibers and protects the fibers from environmental effects. In the late 1940s, the defense and aerospace industries began the development and applications of composite materials to improve the performance and cost-effectiveness of aircraft-type structures. Nowadays, civil engineers are interested in exploiting composite materials in structural applications by taking advantage of their high strength-to-weight ratio, resistance to chemical and environmental corrosion, fatigue resistance, formability to complex shapes, and relatively low cost.

The flexibility of manufacturing process and material combinations make it easy to customize the final product to suit a particular application. The simplest method is the hand lay-up process where sheets of fabric are bonded by hand to the surface of the wall using appropriate resins. This procedure allows the fibers to be oriented in the desired direction to carry the expected loading.

A surface treatment retrofitting technique was investigated by Ehsani and Saadatmanesh (1990) at The University of Arizona. The testing evaluated flexural strengthening of concrete beams by epoxy-bonding glass-fiber-reinforced polymer (GFRP) laminates to the tension face of the beam. The strength of the investigated beams increased significantly. A similar test was conducted by the same researchers on masonry beams to investigate the out-of-plane strength of clay brick masonry walls (Ehsani et al. 1993). In both cases, this method proved to be very effective and a significant increase in strength was observed. This new technique is attractive as it does not require the removal of existing masonry and requires very little surface preparation or formwork. Furthermore, the light weight of FRP eliminates the need for foundation adjustments.

While the use of FRP as an external overlay has been successfully demonstrated in strengthening beams for out-of-plane (flexure) loading, little attention has been given to the use of composites for enhancing the in-plane shear capacity of URM walls. Innamorato (1994) tested these reinforced-concrete masonry wall panels to examine the effectiveness of a repair scheme consisting of a carbon fiber, polymeric matrix composite overlay. Each specimen was tested twice: first, to create the desirable failure mechanism, then repaired with an FRP laminate and retested to evaluate the performance of the composite repair scheme. It was observed that the overall flexural, shear strength, and stiffness quantities were significantly increased with the application of the composite repair. Similar results have been observed in a study conducted in Switzerland, where URM walls were strengthened with carbon FRP (CFRP) sheets and polyester fabric (Schwegler 1994).

The study presented in this paper investigates the effectiveness of using FRP overlays bonded to the surface of solid clay bricks in enhancing the shear strength of these elements.

EXPERIMENTAL STUDY

Test Specimens

Thirty seven specimens were constructed using 64 × 102 × 216 mm (2.5 × 4 × 8.5 in.) clay bricks. The designation for the test specimens starts with the letter "A," followed by a combination of letters/numericals, each describing a variable in the study. The first numerical, 10, 12, or 18, refers to the density of the fabric in oz/sq yd. The letters "L" or "S" following the numerical refer to the length of the fabric as defined in Fig. 2. The letter L is used for the longer fabric [L = 203 mm (8 in.)] and the letter S for the shorter fabric [L = 140 mm (5.5 in.)]. The last numerical, 45 or 90, represents the fiber orientation with respect to the direction of the applied load. For example, the designation A10-L-45 means the composite laminate (overlay) consists of a 10 oz/sq yd (339 gm/m^2) fabric that is 203 mm (8 in.) long with fibers oriented at 45–135° with respect to the applied load direction.

Each specimen consisted of three clay bricks with the middle brick elevated from its base by 51 mm (2 in.) (Fig. 2). To simulate a damaged mortar bed joint, a piece of 3/8-in.-thick plywood was sandwiched between the bricks. The plywood was lubricated to produce nearly a frictionless surface. Thus, in this conservative approach, the detrimental effect of the gap between bricks on the shear strength of FRP was included, while the contribution of the mortar to the shear resistance was totally ignored. The plywood was mounted to the inner

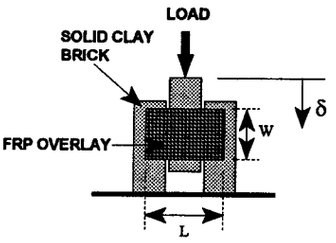

(a)

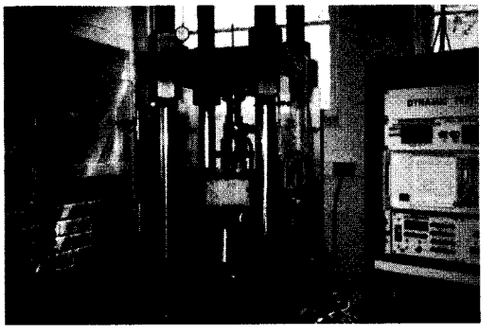

(b)

FIG. 2. (a) Test Specimen; (b) Test Setup

TABLE 1. Mechanical Properties of GFRP Laminate

Fabric Designation Density gm/m² (oz/sq yd)	A10 339 (10)		A12 406 (12)		A18 610 (18)	
Sample number (1)	σ [MPa (ksi)] (2)	E [GPa (ksi)] (3)	σ [MPa (ksi)] (4)	E [GPa (ksi)] (5)	σ [MPa (ksi)] (6)	E [GPa (ksi)] (7)
1	64.1 (9.3)	3.1 (456)	82.0 (11.9)	3.93 (570)	107.0 (15.5)	5.2 (755)
2	60.0 (8.7)	2.9 (426)	73.8 (10.7)	3.86 (560)	106.0 (15.3)	5.2 (756)
3	64.1 (9.3)	3.3 (483)	77.2 (11.2)	3.75 (545)	—	—
Average	32.7 (9.1)	3.1 (455)	77.9 (11.3)	3.85 (558)	106.0 (15.4)	5.2 (754)

face of the bricks by a tape that held the plywood in place but had no strength. The fabric was then bonded to both sides of the bricks using an epoxy of medium viscosity that could be spread easily. The specimen assembly is shown in Fig. 2.

Fabrication

The specimens were fabricated by first cleaning the surface of the bricks from any dust. A wire brush was used to roughen the surface for better adhesion between the brick and the fabric. The plywood boards were taped to the inner surface of the bricks. The bricks were then laid on their narrow face and clamped together after they were aligned in the final position. A mastic tape was attached parallel to the gap between the bricks to prevent any epoxy penetration between the bricks. The epoxy was spread over the clean surface of the brick by an adhesive spreader. Finally, the fabric was laid on top of the epoxy and pressed firmly to ensure adequate saturation and uniform distribution of the epoxy. The same was repeated to the other side of the assemblage after the FRP composite overlay was cured. Two lengths of fabric [L = 203 mm (8 in.) and L = 140 mm (5.5 in.)] were used to observe the effect of anchorage length in the development of the full strength of the fabric. The width of the fabric, W, was 114 mm (4.5 in.) in both cases (Fig. 2).

Materials

Standard clay bricks were used for all test specimens. Three brick units were tested to determine their compressive strength. Their compression strength was found to be 41.5, 44.3, 41.7 MPa (6,020, 6,430, 6,040 psi), respectively, resulting in an average compressive strength of 42.5 MPa (6,160 psi). The woven fabric consisted of bidirectional continuous fibers with equal density in both directions. Three different densities were used in this study. The fabric densities are listed in Table 1. The epoxy used was selected after testing several types for their strength and workability. This epoxy was found to be the most suitable for the current application. It consists of two components mixed to form a paste-like compound that was easily applied to the brick surface. The required curing time of the epoxy was 24 hours at room temperature. In this application, the fabric and the epoxy form an FRP composite laminate. Three samples of each type of composite laminate used in this study were tested under uniaxial tension according to ASTM D3039. The results showed a linear-elastic behavior up to failure. The values of the average modulus of elasticity and ultimate tensile strength are summarized in Table 1. These values are very low because the method of construction does not allow for a high volume of fibers in the finished laminate product.

Instrumentation

The specimens were loaded in a displacement-controlled mode at a rate of 0.0305 mm/s (0.0012 in./s). The displacement of the top of the middle brick relative to the other bricks was measured using a linear variable differential transducer (LVDT) and was recorded automatically. The load was measured using a 44.5 kN (10 kip) load cell.

Test Procedure

The specimens were tested under static loading as shown in Fig. 2(a). The specimens were positioned in a clamping device consisting of two steel side plates and four rollers. The specimens were positioned in the device and the rollers were adjusted to touch the surface of the fabric. The rollers did not provide any resistance in the loading direction (i.e., vertical direction); however, they restrained rotation of the middle brick in the transverse direction (i.e., perpendicular to the plane of the laminate).

In the case of a wall retrofitted with FRP laminates, (1) can be modified as given below:

$$\tau_b = \nu_{b0} + \mu\sigma_y + \tau_{FRP} \tag{2}$$

where τ_{FRP} = contribution of the FRP laminate in resisting

TABLE 2. Description of Test Specimens

Specimen type (1)	Specimen number (2)	Fabric weight [gm/m² (oz/sq yd)] (3)	Fabric length [mm (in.)] (4)	ϕ (°) (5)	P_{max} [kN (kip)] (6)	δ at P_{max} [mm (in.)] (7)	Mode of failure[a] (8)
A10-L-90	1	339	203	90	19.6 (4.4)	7.0 (0.275)	S
	2	(10)	(8)		18.2 (4.1)	4.57 (0.18)	S
	3				17.8 (4.0)	4.83 (0.19)	S
A10-S-90	1	339	140	90	18.7 (4.2)	2.03 (0.08)	DE
	2	(10)	(5.5)		23.6 (5.3)	2.08 (0.082)	S-DE
	3				18.2 (4.1)	1.8 (0.071)	S-DE
A10-L-45	1	339	203	45	19.6 (4.4)	7.2 (0.285)	S
	2	(10)	(8)		16.5 (3.7)	8.4 (0.331)	S
	3				15.6 (3.5)	6.7 (0.265)	S
A12-L-90	1	406	203	90	17.4 (3.9)	9.0 (0.355)	DM
	2	(12)	(8)		16.0 (3.6)	7.6 (0.30)	S-DM
	3				15.6 (3.5)	6.1 (0.24)	DM
A12-L-45	1	406	203	45	21.1 (4.75)	2.2 (0.085)	DM
	2	(12)	(8)		20.5 (4.6)	3.2 (0.120)	DM
	3				20.0 (4.5)	2.6 (0.103)	DM-DE
A18-L-90	1	609	203	90	19.1 (4.3)	9.3 (0.367)	DM
	2	(18)	(8)		16.9 (3.8)	8.9 (0.350)	DM
	3				16.5 (3.7)	7.6 (0.30)	DM
A18-S-90	1	609	140	90	21.4 (4.8)	1.96 (0.077)	DE
	2	(18)	(5.5)		17.8 (4.0)	1.50 (0.060)	DE
	3				16.8 (3.75)	2.0 (0.08)	DE
A18-L-45	1	609	203	45	14.2 (3.2)	7.1 (0.28)	DM
	2	(18)	(8)		13.8 (3.1)	5.8 (0.23)	DM-DE
	3				15.1 (3.4)	6.4 (0.25)	DM

[a]S = shear failure along the joint, DM = delamination of fabric at middle-brick region, and DE = delamination of fabric edges at the outer bricks.

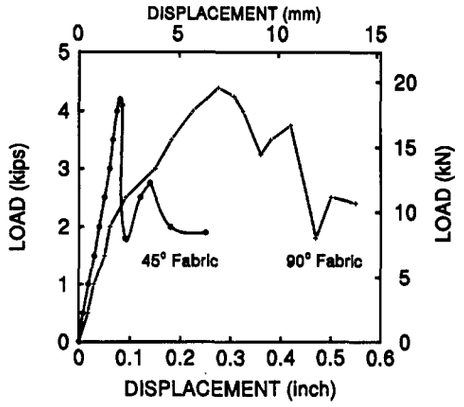

FIG. 3. Typical Load versus Displacement Graph

shear. In this study, the bed joint is assumed to be $\nu_{b0} = 0$. This assumption is valid as long as the bed joint is cracked (i.e., bond is destroyed) and a separation between the bricks has occurred. Also, the normal stress was intentionally set equal to zero (i.e., $\sigma_y = 0$) to eliminate any frictional force generated by the relative movement of the bricks under the applied shear load. Of course, these assumptions are very conservative. In real field conditions, normal stresses are provided by the weight of the wall and other gravity loads applied on the shear wall that may be present. In addition, the shear bond will always provide some shear resistance since cracks do not extend along the whole wall. The conservative approach followed in this study proves the effectiveness of this technique in strengthening a bed joint that is assumed to have no strength at all. Thus, the entire load-carrying capacity in each test specimen was attributed to τ_{FRP} only.

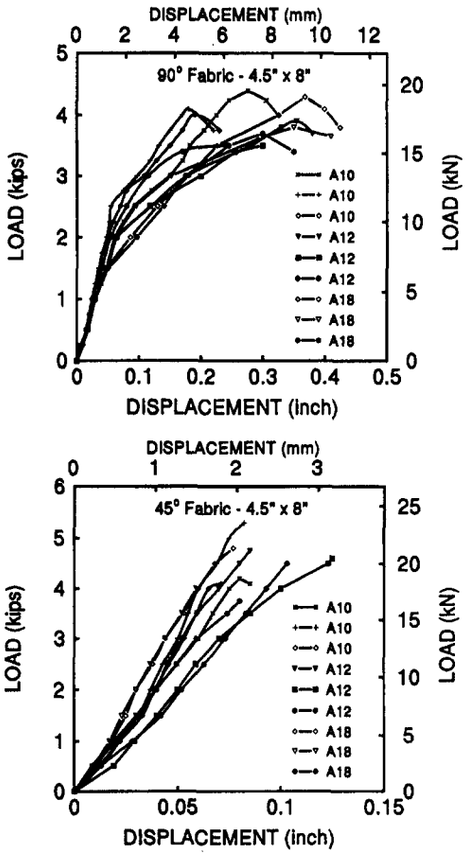

FIG. 4. Effect of Fabric Density on Ultimate Load

Design Variables

The design variables considered in this study included the strength of the fabric, the orientation of the fibers, and the anchorage length of the fabric. As discussed earlier, fabrics with three different strengths (densities) were investigated to observe their effect on the modes of failure. In fiber composites, the orientation of the fiber influences both the strength and stiffness as will be shown in the discussion of the test results. The fibers of the fabric were oriented at 0–90° or 45–135° to the direction of the applied load. Finally, the

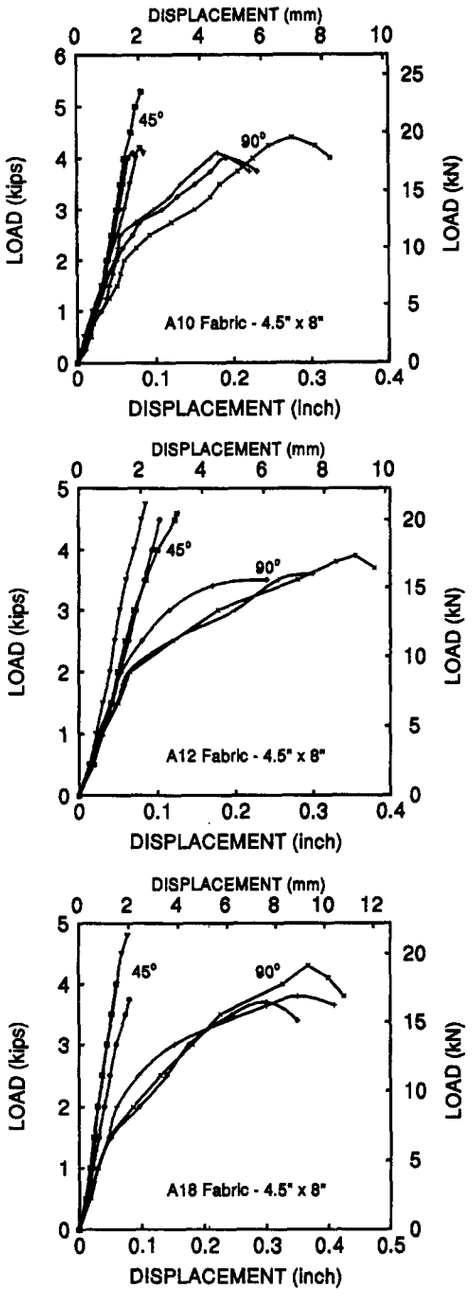

FIG. 5. Effect of Fiber Orientation: (a) A10 Fabric; (b) A12 Fabric; (c) A18 Fabric

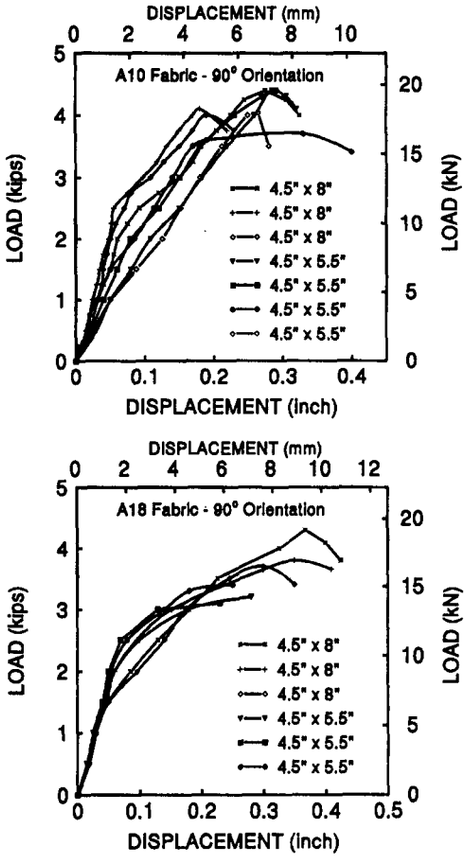

FIG. 6. Effect of Fabric Length on Ultimate Load

length of the fabric [203 mm (8 in.) or 140 mm (5.5 in.)] was selected to examine its effect on the development of the full strength of the fabric.

Test Results and Comment

The description of test specimens is summarized in Table 2. Typical measured load versus displacement of the top of the middle brick for specimens with the fibers oriented at 45 and 90° are shown in Fig. 3. As can be seen several load peaks are presented in the descending portion of each graph. For clarity, it was decided to report each graph only up to the ultimate (peak) load value. The load versus displacement curves for 24 specimens that were considered for the analysis are presented in Figs. 4–6.

Modes of Failure

Two modes of failure were observed. The failure was dependent on the fabric strength and length. In the case of A10-L-90 and A10-L-45 specimens, the failure was a direct (simple) shear along one of the joints and the fibers were sheared completely along the joint. For fabrics with higher density, the failure was due to delamination of fabric (i.e., bond failure) at the middle-brick region. In this case the middle brick was sliding easily once the peak value was reached and debonding of the fabric was initiated at one side. On the other hand, A10-S-90 specimens, with a shorter fabric, showed a combined shear failure at the joint and delamination of the fabric at the outer edges. The failure in the case of A18-S-90 was due to delamination of fabric edges at the outer bricks.

Effect of Fabric Strength (Density)

Failure of A10-L-90 specimens was initiated by simple shear along one of the joints as shown in Fig. 7. At this point the peak value was reached and the load dropped gradually due to progressive breaking of the fibers along the joint. The load then started to rise again due to the resistance provided by the fabric at other joints. This was usually followed by a few other localized peaks until the final failure of the specimen. In most cases the delamination (debonding) was caused by lateral displacement of the middle brick, which could rotate and push against the opposite side (i.e., unfailed) fabric.

Failure of the A12-L-90 and A18-L-90 specimens was a result of delamination of fabric at the middle-brick region. This type of failure prevented development of the full strength of the fabric, which was expected to be higher than that of A10-L-90. This clearly indicates that bond and contact area between the brick and the fabric is very crucial in order to

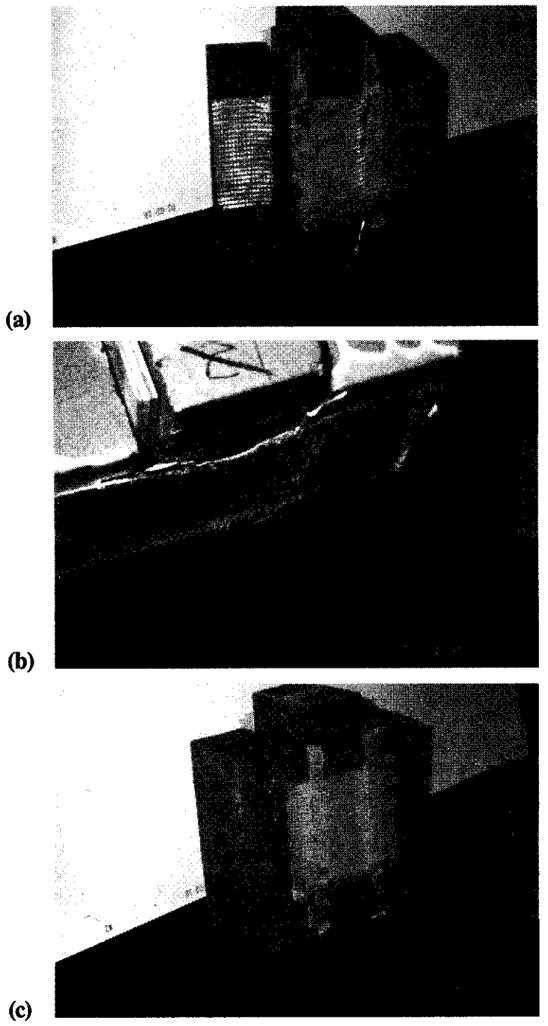

FIG. 7. Modes of Failure: (a) Shear Failure; (b) Delamination of Fabric at Middle Brick; (c) Delamination of Fabric Edges

develop the full strength of the composite material. Since the load on the middle brick is twice that of the outer bricks and considering the equal bond area on all three bricks, it can be said that stresses developed at the middle brick are twice those of the outer bricks. As can be seen in Fig. 4, the stiffness for the specimens decreased as the fabric density increased. This is contrary to the expected behavior. However, as the density of the fabric increased, a thorough wet out of the fabric with epoxy became more difficult to achieve. As a result, some portions of the higher-density fabrics were not properly bonded to the bricks. This resulted in failure by debonding of the fabric from the more highly stressed middle bricks in these specimens.

Furthermore, it was observed that the initial stiffness up to a load value of 8.9 kN (2 kips) was nearly the same for all specimens regardless of the fabric density. The stiffness then decreased with the increase of the fabric density as shown in Fig. 4. This is attributed to the wet-out problem explained earlier.

Effect of Fiber Orientation

Two fiber orientations were investigated in this study, namely 90 and 45° with respect to the load direction. The load versus displacement curves of A10, A12, and A18-L-90 and A10, A12, and A18-L-45 specimens are compared in Fig. 5. In most cases the ultimate load of the 45° orientation slightly exceeded that of the 90° orientation for the same fabric density. In addition, the displacement at the ultimate load in the 45° case was between 20–30% of that for the 90° fiber orientation.

The 45° oriented fabric showed almost a constant stiffness throughout the loading range. On the other hand, for the 90° orientation the stiffness was initially constant and decreased gradually. At the ultimate load the stiffness was theoretically zero (i.e., slope of the tangent to the curve was zero). Beyond the ultimate load, the stiffness was negative due to the drop in the strength. The load was then redistributed and a positive stiffness was observed until the second peak was formed and the same was repeated until a complete failure occurred.

The constant and higher stiffness observed in the case of the 45° oriented fiber has as important design implication. It was pointed out that the ultimate load was reached at a very small displacement of approximately 2.5 mm (0.1 in.) compared to 7.5 mm (0.3 in.) in the case of the 90° fiber orientation. The higher stiffness is very desirable where deformation of the shear wall is to be kept small while attaining the maximum strength in the fabric; an example is shear walls with window openings. Excessive deformation to develop the full strength of the fabric may cause damage to the windows. Similarly, in infill frames, the presence of the frame may limit the wall displacement. Therefore, it will be desirable to resist large forces within the small deformation of the wall. In these cases, orienting the fibers at 45° will be very advantageous. In the case of 90° fabrics, a more ductile failure was observed; a combination of both orientations can result in a stiff system with some ductility.

Effect of Fabric Length

A shorter fabric, 14 × 11.5 mm (5.5 × 4.5 in.), was used to examine its influence on the strength. This length was used in A10-S-90 and A18-S-90 specimens. No specimens with short A12 fabrics were tested. As shown in Fig. 6(a), the ultimate load in the case of A10-S-90 and A10-L-90 specimens is almost the same for both fabric lengths. Also, it was observed during testing that the failure was due to a combination of delamination of the fabric at edges and shear failure at one of the joints. This indicates that the shorter length is sufficient to develop the full strength of the fabric. On the other hand, a difference in strength was observed in the case of A18-S-90 and A18-L-90 specimens as shown in Fig. 6(b). The failure of the specimens with shorter fabrics was due to delamination of fabric edges compared to delamination at the middle brick for specimens with long fabrics. The fabric failed in this manner since the fabric covered only 29 mm (1.12 in.) of the outer bricks from the joints while the longer fabric covered the full width of the outer bricks. This indicates the significance of anchorage (development) length in developing the full strength of the material.

ANALYTICAL STUDY

The behavior of composite laminates is highly dependent on the orientation of fibers and type of loading. Mallick (1988) reported that the tensile stress-strain relation for glass-fiber-composite laminate according to ASTM D3039 is almost linear up to failure. The same was confirmed for the various fiber densities used in this study as shown in Fig. 8(a). However, the shear stress-strain relation is nonlinear, as shown in Fig. 8(b) (Mallick 1988; Vinson and Sierakowski 1987). The same behavior was observed for fabric with 90° fiber orientation, as shown previously in the test results, where the fibers along the joints were stressed in shear. To understand the experimental results the stresses along the joints (failure plane) were analyzed using finite-element method (FEM) analysis and basic composite mechanics as discussed in the following sections.

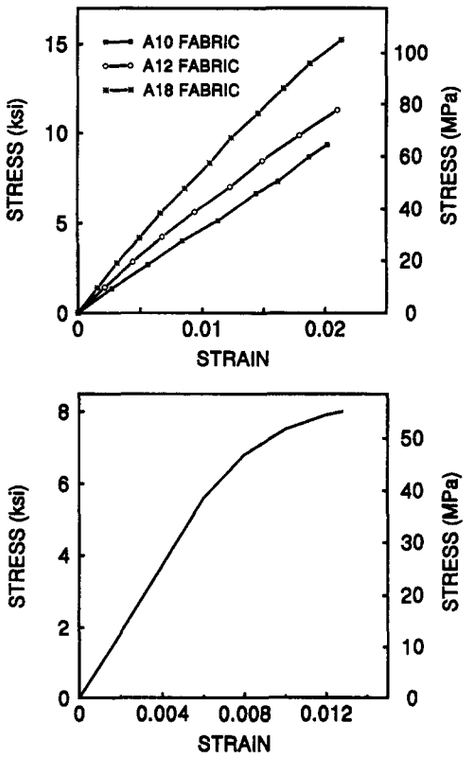

FIG. 8. Tensile and Shear Stress-Strain Relationship of GFRP Lamina

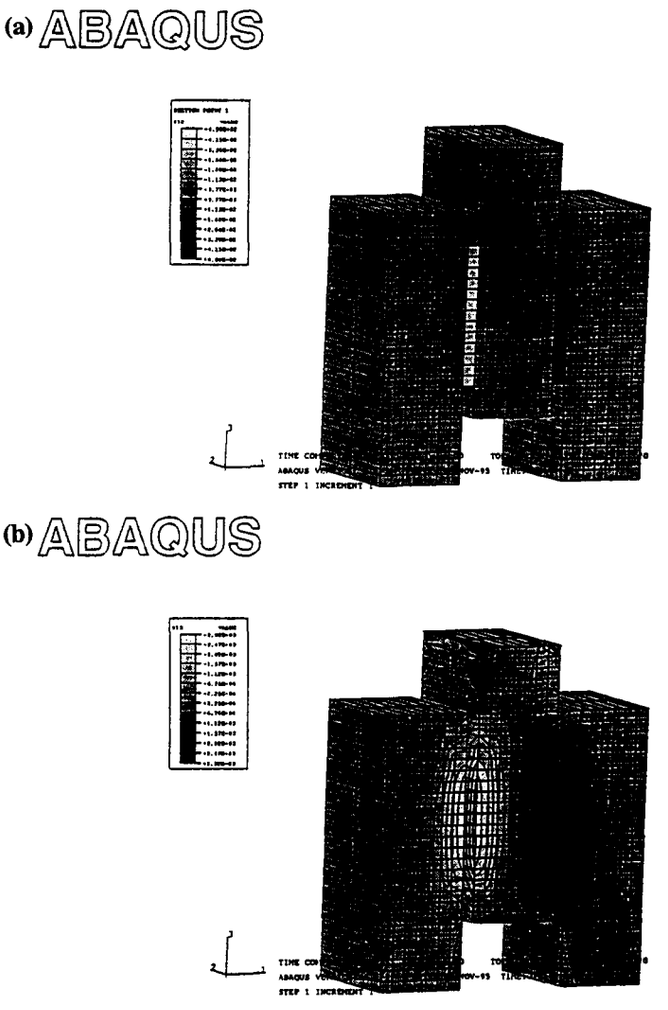

FIG. 9. Stress Contour in Test Specimen

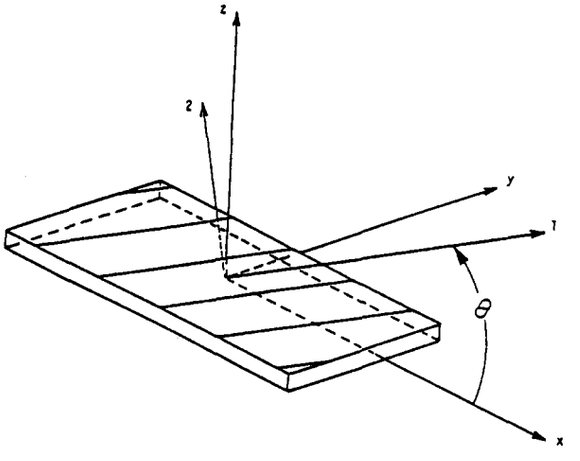

FIG. 10. Definition of Stress Transformation in a Laminate

The stress distribution in the test specimens were obtained using the ABAQUS finite-element program. The bricks were modeled using three-dimensional (3D) solid elements with eight nodes, and the fabric was modeled using four node shell elements assuming a thick shell with the specified dimension of elements (Cook 1981; Gaylord and Gaylord 1990). The specimens were discretized to a total of 1,700 nodes and 1,680 elements. A linear-elastic material behavior was assumed since the brick was stressed within the linear limit. Only a 45° fiber orientation was considered and the behavior was assumed to be linear up to failure. A perfect bond between the fabric and the brick surface was also assumed in this study.

Based on the foregoing assumptions only A10-L-45 fabric was considered for analysis since the failure was caused by direct shear along the joints (failure plane) and not due to delamination (bond failure); the response of this specimen can be assumed to be linear-elastic. The FEM analysis revealed that the shear stresses in the fabric τ_{12} were uniformly distributed along the joints. The shear stress contours in the test specimen are shown in Fig. 9. From the figures, it can be noticed that the shear stress in the fabric [Fig. 9(a)] is uniformly distributed while the shear stresses in the brick elements [Fig. 9(b)] are maximum at the middle third of the joint and decrease gradually towards the ends of the joint.

To understand the different response obtained from experimental results for 90 and 45° fiber orientation, basic principles of mechanics for composite materials were used along with the stress distribution obtained from the finite-element analysis. In fiber composites two right-handed coordinate systems are considered in the analysis of any laminate. These are the 1-2-z and x-y-z systems as shown in Fig. 10. Both the 1-2 and x-y axes are in the plane of the laminate, and the z-axis is normal to this plane. In the 1-2-z system, 1 and 2 are associated with the fiber direction in the laminate and are usually defined as the principal material axes. In the x-y-z, x and y represent the loading direction. The angle between the positive x-axis and the 1-axis is called the fiber orientation angle and is represented by θ.

Since the behavior of fiber composites is more easily understood in terms of their material principle axes, the following equations are useful in transforming stresses from the x-y direction (loading axes) to stresses in the 1-2 direction (Mallick 1988):

$$\sigma_{11} = \sigma_{xx} \cos^2\theta + \sigma_{yy} \sin^2\theta + 2\tau_{xy} \cos\theta \sin\theta \quad (3a)$$

$$\sigma_{22} = \sigma_{xx} \sin^2\theta + \sigma_{yy} \cos^2\theta - 2\tau_{xy} \cos\theta \sin\theta \quad (3b)$$

$$\tau_{12} = (-\sigma_{xx} + \sigma_{yy})\sin\theta \cos\theta + t_{xy}(\cos^2\theta \sin^2\theta) \quad (3c)$$

where σ_{xx}, σ_{yy}, and τ_{xy} are applied stresses in the x-y directions; and σ_{11}, σ_{22}, and τ_{12} are transformed stresses in the 1-2 directions. To apply the foregoing equations to this problem, an element at the joint (failure plane), as shown in Fig. 11, was analyzed for both fiber orientations [i.e., 90 and 45° to the direction of the applied load (y-axis)]. The 90° orientation to the applied load (y-axis) is the same as $\theta = 0°$ (i.e., direction with respect to the x-axis).

Fig. 12(a) shows the case for the fibers oriented at 90° (i.e., $\theta = 0°$). Assuming that the element is under pure shear stress τ_{xy} and $\sigma_{xx} = \sigma_{yy} = 0$, (3) leads to $\sigma_{11} = 0$, $\sigma_{22} = 0$, and $\tau_{12} = \tau_{xy}$. With the fibers oriented at 45° (i.e., $\theta = 45°$) as shown in Fig. 12(b), the same assumptions result in $\sigma_{11} = \tau_{xy}$, $\sigma_{22} = -\tau_{xy}$, and $\tau_{12} = 0$.

Looking at the transformed principal stresses it was noted that in the case of $\theta = 0°$ the fibers were under pure shear. As mentioned earlier, the behavior of fiber composite laminates under shear stress is nonlinear. The experimental results supports this behavior where all tested specimens with a 90° fiber demonstrated a nonlinear response. However, in the case of $\theta = 45°$ the main fibers were under axial tension. This also agrees with the experimental results where the specimens showed almost a linear behavior, which is characteristic of fiber composite laminates under uniaxial tension. The average tensile strength according to ASTM standard test was 62 N/mm^2 (9 ksi) and the experimental stress values, σ_{11}, according to the preceding equations was 45 N/mm^2 (6.5 ksi). This

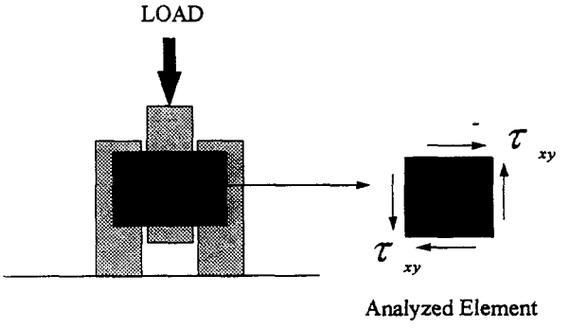

FIG. 11. Typical Stresses in a Joint Element

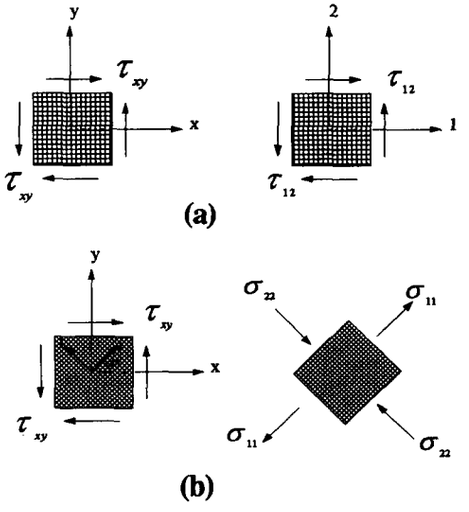

FIG. 12. Transformation of Stresses for: (a) θ = 0°; (b) θ = 45°

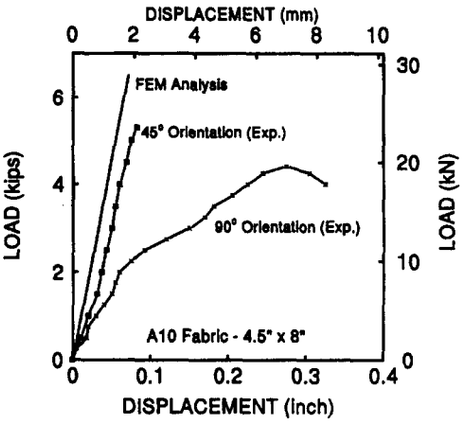

FIG. 13. Comparison of FEM and Experimental Results

apparent lower strength is mainly due to the fact that the lack of normal stresses allowed the bricks to move outward at the base. This caused some bending stresses on the fabric, resulting in additional tension on the bottom fibers at the joints. In this case, the bottom fibers were stressed more than those calculated from (3).

The load versus displacement obtained from FEM is compared with the experimental results in Fig. 13. The predicted load versus displacement curve is compatible with the experimental results in the case of the 45° fiber orientation. The slight difference in the slope is attributed to the imperfect bond between the brick and the laminate in the test specimens; the FEM solution assumed perfect bond. The measured response is linear as was assumed in the analysis. There is clearly a difference between the FEM solution and the experimental results for specimens with 90° fabrics. It was shown that fibers oriented at 90° were stressed in shear, hence the response was expected to be nonlinear. Thus, the FEM model that assumes linear behavior for the FRP laminates is only valid for specimens with fibers oriented at 45°.

SUMMARY AND CONCLUSIONS

The experimental study involved construction and testing of 37 clay brick specimens with FRP overlays. Three different fabric densities were used and the fiber orientation as well as the fabric length were varied to observe their effect on the developed strength. Two modes of failure were observed: (1) shear failure along the bed joint; and (2) delamination of fabric at the middle-brick region or fabric edges. The type of failure was influenced by the fabric strength. Shear failure was observed in the case of A10-L-90 fabric and bond failure in A12-L-90.

The strength and stiffness of the specimens were highly influenced by the fiber orientation. Changing the fiber orientation from 90 to 45° led to a slight increase in the ultimate load. Moreover, the stiffness of A10, A12, and A18-L-45 specimens was almost constant during the entire range of loading, with displacement at the ultimate load being 20–30% of that of A10, A12, and A18-L-90 specimens. In addition, the fabric length was very important in the strength development. This indicates that in order to develop the full strength of the material, a sufficient fabric length is required. In the case of A10 fabric, the shorter length [L = 140 mm (5.5 in.)] was adequate, but the same was not true in the case of A18 fabric. The test results proved indisputably that FRP overlays can be very effective in strengthening bed joints of URM walls. The ease of application and relatively low cost makes this technique a viable alternative to current practices.

ACKNOWLEDGMENTS

Partial financial support for this study was provided under National Science Foundation (NSF) Grant No. CMS-9421950. The views expressed in this paper are those of the writers and do not necessarily represent the views of the sponsor.

APPENDIX I. REFERENCES

Abrams, D. P. (1992). "Strength and behavior of unreinforced masonry element." *Proc., 10th World Conf. on Earthquake Engrg.*, A. A. Balkema, Rotterdam, The Netherlands, 3475–3480.

Amrhein, J. E. (1992). *Reinforced masonry engineering handbook.* Masonry Inst. of Am., Los Angeles, Calif.

Chen, H. L., and Shah, S. P. (1988). "Test of model masonry single pier under dynamic shaking and quasi-static cyclic loading." *Masonry: materials, design, construction, and maintenance, ASTM STP 992*, H. A. Harris, ed., ASTM, Philadelphia, Pa., 145–165.

Cook, R. D. (1981). *Concepts and applications of finite element analysis.* John Wiley & Sons, Inc., New York, N.Y.

Drysdale, R. G., Vanderkyle, R., and Hamid, A. (1979). "Shear strength of brick masonry joints." *Proc., 5th Int. Brick Masonry Conf.*, Brick Inst. of Am., Reston, Va., 160–113.

Drysdale, R. G., Hamid, A., and Baker, L. R. (1994). *Masonry structures, behavior and design.* Prentice Hall, Inc., Englewood Cliffs, N.J., 223–230.

Ehsani, M. R., and Saadatmanesh, H. (1990). "Fiber composite plates for strengthening bridge girders." *Int. J. of Compos.*, 15(4), 343–355.

Ehsani, M. R., Saadatmanesh, H., Abdelghany, I. H., and Elkafrawy, W. (1993). "Flexural behavior of masonry walls strengthened with composite fabrics." *Proc., ACI Int. Symp. on Non-Metallic Continuous Reinforcement*, Am. Concrete Inst. (ACI), Detroit, Mich., 497–507.

Gaylord, E. H., and Gaylord, C. N. (1990). *Structural engineering handbook*, 3rd Ed., McGraw-Hill Book Publishing Co., Inc., Section 1, 46–77.

Innammorato, D. (1994). "The repair of reinforced structural masonry walls using a carbon fiber, polymeric matrix composites overlay," ME thesis, Univ. of California, San Diego, Calif.

Jabarov, M., Kozharinov, S. V., and Lunyov, A. A. (1980). "Strengthening of damaged masonry by reinforced mortar layers." *Proc., 7th World Conf. on Earthquake Engrg., Vol. 4*, Turkish Nat. Committee, Ankara, Turkey, 73–80.

Kahn, L. F. (1984). "Shotcrete strengthening of brick masonry walls." *Concrete Int.*, 6(7), 34–40.

Lenczner, D. (1972). *Element of load bearing brickwork.* Pergamon Ltd., Oxford, England, 18–38.

Mallick, P. K. (1988). *Fiber reinforced composites, materials, manufacturing and design.* Marcel Dekker, Inc., New York, N.Y.

Prawl, S. P., Reinhorn, A. M., and Kunnath, S. K. (1986). "Seismic strengthening of structural masonry walls with external coatings." *Proc., 3rd U.S. Conf. on Earthquake Engrg., Vol. 2*, Earthquake Engrg. Res. Inst. (EERI), El Cerrito, Calif., 1323–1333.

Reinhorn, A. M., Prawl, S. P., and Jia, Z.-H. (1985). "Experimental study of ferrocement as a seismic retrofit material for masonry walls." *J. of Ferrocement*, 15(3), 247–260.

Schwegler, G. (1994). "Masonry construction strengthened with fiber composites in seismically endangered zones." *Proc., 10th Eur. Conf. on Earthquake Engrg.*, A. A. Balkema, Rotterdam, The Netherlands, 454–458.

Sheppard, P., and Tercelj, S. (1980). "The effect of repair and strengthening methods for masonry walls." *Proc., 7th World Conf. on Earthquake Engrg., Vol. 6*, Turkish Nat. Committee on Earthquake Engrg., Ankara, Turkey.

Vinson, J. R., and Sierakowski, R. L. (1987). *The behavior of structures composed of composite materials.* Martinus Nijhoff Publishers, Dordrecht, The Netherlands.

APPENDIX II. NOTATION

The following symbols are used in this paper:

DE = failure mode by delamination of fabric at the outer bricks;
DM = failure mode by delamination of fabric at middle brick region;
E = modulus of elasticity of FRP laminate;
S = failure mode by shear along the joint;
μ = coefficient of friction between brick and mortar;
v_{b0} = shear bond strength at zero normal stress due to the adhesive strength of mortar;
σ = tensile strength of FRP laminate;
σ_y = normal stress;
τ_b = shear stress at shear bond failure;
τ_{FRP} = contribution of the FRP laminate in resisting shear; and
ϕ = orientation of fibers with respect to the load direction.